

Cite this: *Chem. Sci.*, 2022, 13, 241

All publication charges for this article have been paid for by the Royal Society of Chemistry

Received 17th November 2021  
Accepted 6th December 2021

DOI: 10.1039/d1sc06403g

rsc.li/chemical-science

# Photocatalytic synthesis of tetra-substituted furans promoted by carbon dioxide†

Ya-Ming Tian, Huaiju Wang, Ritu and Burkhard König \*

We report a simple protocol for the transition metal-free, visible-light-driven conversion of 1,3-diketones to tetra-substituted furan skeleton compounds in carbon dioxide (CO<sub>2</sub>) atmosphere under mild conditions. It was found that CO<sub>2</sub> could be incorporated at the diketone enolic OH position, which was key to enabling the cleavage of a C–O bond during the rearrangement of a cyclopropane intermediate. This method allows for the same-pot construction of two isomers of the high-value tetra-substituted furan scaffold. The synthetic scope and preliminary mechanistic investigations are presented.

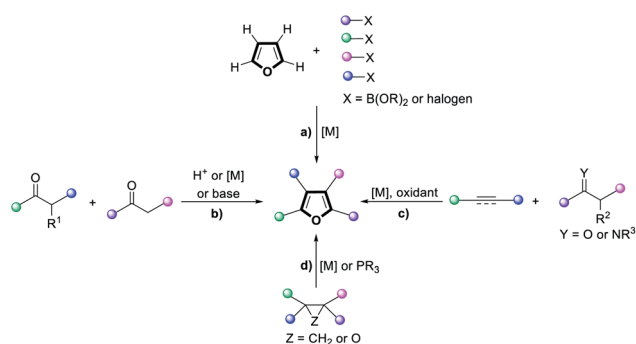
## Introduction

Polysubstituted furans are of great importance in the flavor and fragrance industry, pharmaceutical industry and materials chemistry, and are also valuable building blocks in organic synthesis.<sup>1</sup> However, the preparation of such polysubstituted furans is often complicated and circuitous. While direct functionalization of the furan C–H positions is possible (Scheme 1a), regioselectivity challenges and detrimental reactivity of the furan ring itself hampered such approaches. Classical strategies to construct fully functionalized furans include the Feist–Benary reaction<sup>2</sup> and Paal–Knorr condensation<sup>3</sup> (Scheme 1b).

Annulation of unsaturated substrates with ketones or imines<sup>4</sup> (Scheme 1c) as well as other cross-coupling approaches<sup>5</sup> could also afford polysubstituted furans, but migratory cycloisomerization<sup>6</sup> and rearrangements<sup>7</sup> are the most straightforward and convergent routes (Scheme 1d).<sup>8</sup> Furthermore, current methods to access such furans typically require the use of metal catalysts and multiple components. As such, an atom-efficient, transition metal-free, organocatalytic protocol to synthesize tetra-substituted furans from a single precursor is highly sought after.

Carbon dioxide as a natural, abundant, inexpensive, easy-to-separate, and recyclable C1 building block has become the focus of recent research,<sup>9–11</sup> but its capability to catalytically promote reactions has not been widely explored. Shell Oil Company first patented the utilization of CO<sub>2</sub> to facilitate the synthesis of propionaldehydes in 1968,<sup>12</sup> but only in 2007 was a CO<sub>2</sub>-catalyzed rearrangement of propargyl alcohols to unsaturated ketones reported by Yamada (Scheme 2a).<sup>13</sup> Proceeding *via* a carbonate intermediate generated between CO<sub>2</sub> and the propargyl alcohol, the reaction regenerates the gas upon formation of the product. Similarly, Tunge showed the use of CO<sub>2</sub> to engage allylic OH groups, producing better leaving groups for cross-coupling (Scheme 2b),<sup>11g</sup> and Das further reported the CO<sub>2</sub>-promoted oxidation of allylic alcohols to unsaturated aldehydes (Scheme 2c).<sup>10b</sup> More recently, it was also demonstrated that CO<sub>2</sub> can act on amine substrates to activate  $\alpha$ -C–H bonds for intermolecular hydrogen atom transfer.<sup>14,15</sup> Taken together, while the study of CO<sub>2</sub>-catalysis is still in its infancy, it offers new opportunities to perform organocatalysis that can complement traditional metal-based chemistry.

Therefore, we envisioned utilizing CO<sub>2</sub> together with organic dyes to catalyze the cyclizations of 1,3-diketones<sup>1b,16,17</sup> and subsequent cyclopropane rearrangement events<sup>7</sup> *en route* to valuable tetra-substituted furan products, enabled by the reversible interaction of CO<sub>2</sub> with the enol forms that can provide favorable carbonate leaving groups.<sup>10b,c,11g</sup> The

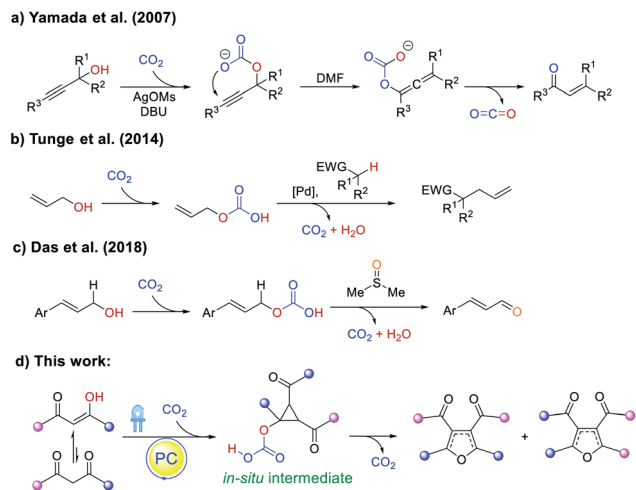


**Scheme 1** Approaches to access highly substituted furans *via*: (a) successive direct functionalization of furan C–H; (b) condensation; (c) annulation of unsaturated substrates with ketones or imines; (d) migratory cycloisomerization and rearrangements.

Institute of Organic Chemistry, Faculty of Chemistry and Pharmacy, University of Regensburg, 93040 Regensburg, Germany. E-mail: Burkhard.Koenig@chemie.uni-regensburg.de

† Electronic supplementary information (ESI) available. CCDC 2113371. For ESI and crystallographic data in CIF or other electronic format see DOI: 10.1039/d1sc06403g





**Scheme 2** CO<sub>2</sub>-promoted organic transformations: (a) rearrangement of propargyl alcohols to unsaturated ketones; (b) cross-coupling using native allylic alcohol; (c) oxidation of allylic alcohols to unsaturated aldehydes. This work: (d) synthesis of tetra-substituted furans.

optimization survey, substrate scope, and preliminary mechanistic studies of this transition metal-free, photocatalytic, and CO<sub>2</sub>-promoted furan synthesis strategy are presented herein.

## Results and discussion

We started our investigation by employing 1-phenyl-1,3-butanedione (**1a**) as the model substrate in the presence of CO<sub>2</sub>. At first, a range of commercially available organic photocatalysts and bases were screened (Table S1<sup>†</sup>). Gratifyingly, the desired tetra-substituted furans were produced by using 4CzIPN as the photocatalyst, *N,N*-dimethylformamide (DMF) as solvent, Cs<sub>2</sub>CO<sub>3</sub> as a base, at 25 °C under 455 nm light irradiation, and in CO<sub>2</sub> atmosphere. Surprisingly, two different tetra-substituted isomers can be formed in the same reaction system, giving 48%

and 50% yield of products **1b** and **1c**, respectively (Table 1, entry 1). Temperature of the photocatalytic reaction seemingly has an effect on the regioselectivity between **1b** and **1c** (Table 1, entry 2). The yields of the products are influenced by the amount of base, with 1.5 equivalents of Cs<sub>2</sub>CO<sub>3</sub> providing the best yields (Table S2<sup>†</sup>). We then screened a range of solvents, with DMF proving to be optimal (Table S3<sup>†</sup>). Light sources at different wavelengths were found to be similarly effective (Table S4<sup>†</sup>). However, when the CO<sub>2</sub> atmosphere was replaced with N<sub>2</sub>, no desired products were formed (Table 1, entry 3). Only trace amounts of products **1b** and **1c** were detected when the reaction was carried out under air (Table 1, entry 4), indicating that CO<sub>2</sub> is an indispensable component in this reaction. In the dark, no reaction occurred at either 25 °C or 60 °C (Table 1, entries 5 and 6), ruling out a base-catalyzed thermal pathway. Similarly, no detectable products were formed when the reaction was carried out in the absence of photocatalyst or base (Table 1, entries 7 and 8).

With the optimized reaction conditions in hand, we evaluated the scope and limitations of this method (Scheme 3). Both electron-rich and electron-deficient phenyl rings were well tolerated (**2–4**, **6**), but a mesityl group provided deleterious steric hindrance (**5**). Diaryl-1,3-diketones reacted smoothly to afford the desired products (**7–9**). Notably, the reaction of **9a** could produce three different products when the two phenyl groups contain different substituents. Other benzene systems such as biphenyl (**10**), phenyl ether (**11**), naphthalene (**12**) and benzodioxane (**13**) were also compatible with our reaction conditions. The preference for the symmetric regioisomers in **2**, **6**, and **10** cannot be explained at the current stage. Furthermore, this method was successfully extended to heterocyclic substituents, such as furan and thiophene (**14**, **15**). Surprisingly, when the 1,3-diketone motif was replaced with 3-oxo-ester, the reaction yielded 2,5-dihydrofurans (**16b**, **17**) and unsymmetric 2,3-dihydrofurans (**16c**, dr > 20 : 1) that resisted regioisomerization and further oxidation to furans even after extensive exposure to air (*vide infra*). We speculate that the less hydridic C2 hydrogens and the overall less electron-rich conjugation systems made **16** and **17** products stable to oxidation, while the electronic effects of the benzene ring could affect the equilibrium between different dihydrofuran isomers (**16c** vs. **17c**). Unfortunately, no reaction occurred with acetylacetone **18a** (*vide infra*). The structure of product **1b** was unambiguously confirmed *via* single crystal X-ray analysis. A gram-scale reaction of **1a** was also conducted under standard conditions, giving 40% and 47% yield of products **1b** and **1c**, respectively.

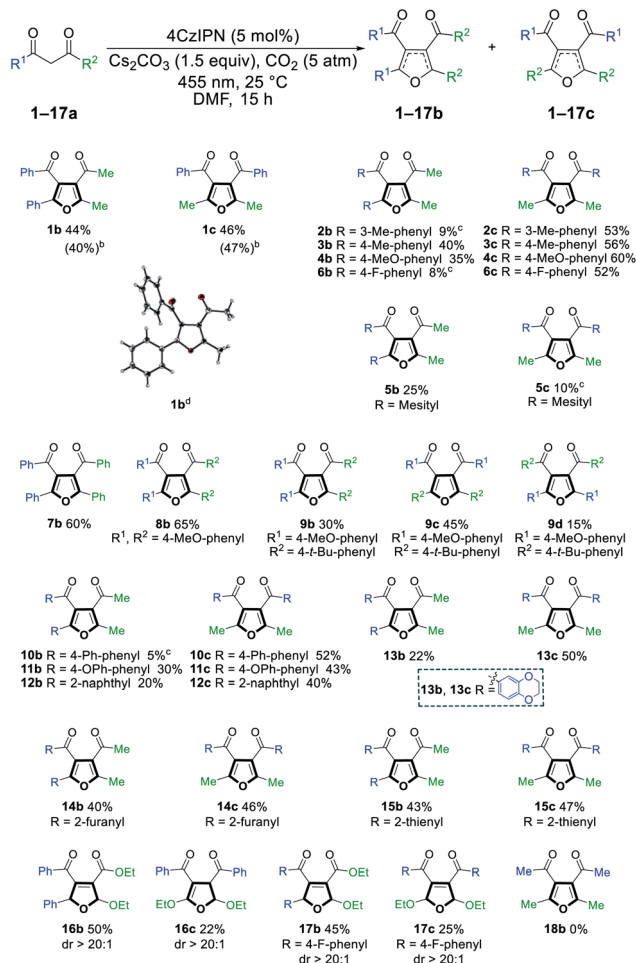
In order to gain insight into the aforementioned transformation, a series of mechanistic studies was conducted. To confirm whether the reaction proceeds *via* a radical process, *in situ* electron paramagnetic resonance (EPR) spectra of different reactions were recorded (Table S6<sup>†</sup> and Fig. S1–S14<sup>†</sup>). No signal was observed for the mixture of **1a**, 4CzIPN, and CO<sub>2</sub>, either with or without blue light irradiation (Table S6,† entries 1 and 2). Similarly, the mixture of **1a**, Cs<sub>2</sub>CO<sub>3</sub>, and CO<sub>2</sub> did not show any signal with or without blue light irradiation (Table S6,† entries 3

**Table 1** Control experiments for the reaction of **1a**

Entry	Deviations from standard conditions	Yield of <b>1b</b> <sup>a</sup>	Yield of <b>1c</b> <sup>a</sup>
1	None	48%	50%
2	60 °C	24%	75%
3	N <sub>2</sub> (1 atm) instead of CO <sub>2</sub>	n.d.	n.d.
4	Air (1 atm) instead of CO <sub>2</sub>	<1%	<1%
5	No light, 25 °C	n.d.	n.d.
6	No light, 60 °C	n.d.	n.d.
7	No 4CzIPN	n.d.	n.d.
8	No Cs <sub>2</sub> CO <sub>3</sub>	n.d.	n.d.

<sup>a</sup> Yields were determined by GC-MS analysis against an internal standard and are the average of two runs; n.d., product was not detected.





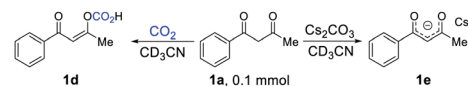
**Scheme 3** Substrate scope of tetra-substituted furan from 1,3-diketone. <sup>a</sup>Reaction conditions: 1,3-diketone (0.5 mmol), 4CzIPN (0.025 mmol), Cs<sub>2</sub>CO<sub>3</sub> (0.75 mmol), CO<sub>2</sub> (5 atm) in DMF (5 mL) at 25 °C under irradiation with a 455 nm LED for 15 h. Reported yields are isolated yields unless stated otherwise. <sup>b</sup>Isolated yields of gram-scale reaction. <sup>c</sup>Yields were determined by GC-MS analysis against an internal standard and are the average of two runs. Products were not isolated due to their low yields. <sup>d</sup>Crystal structure of **1b** as determined by X-ray crystallography at 123 K (see ESI<sup>†</sup>).

and **4**). In addition, there was no EPR signal when mixing 4CzIPN, Cs<sub>2</sub>CO<sub>3</sub>, and CO<sub>2</sub> (Table S6,† entries 5 and 6), or **1a** with CO<sub>2</sub> alone (Table S6,† entries 7 and 8). However, a significant EPR signal was observed when a composition of **1a**, 4CzIPN, Cs<sub>2</sub>CO<sub>3</sub>, and CO<sub>2</sub> was irradiated (Table S6,† entry 10). When the CO<sub>2</sub> atmosphere was replaced with N<sub>2</sub>, the same signal was still present (Table S6,† entry 12), indicating that CO<sub>2</sub> did not participate in the generation of this radical species. To identify the origin of the radical resonance signal, we employed **7a** instead of **1a** in the EPR measurement, obtaining an identical signal (Fig. S7–S9†). Speculating that the signal arose from a 4CzIPN radical anion, we recorded the EPR spectrum of this species by adding NEt<sub>3</sub> as an electron donor to a solution of 4CzIPN (Fig. S14†), which gave the same resonance signal as did the catalysis system.<sup>18</sup> Accordingly, we concluded that **1a**, 4CzIPN, Cs<sub>2</sub>CO<sub>3</sub> and light irradiation together resulted in the

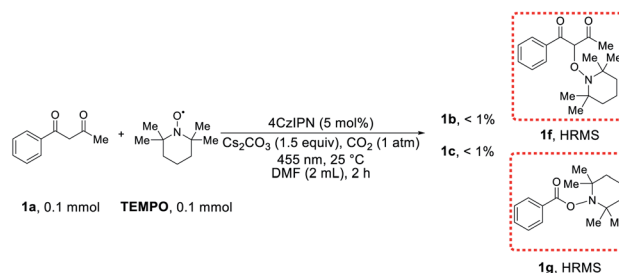
formation of 4CzIPN radical anion. Then, the redox behavior of **1a** and its anion **1a**<sup>−</sup> were investigated. For **1a**, no oxidation peak was observed within the electrochemical window of DMF as solvent (Fig. S15†). The anion of **1a**, synthesized independently, showed an irreversible one-electron oxidation ( $E_{\text{ox}} = -0.09$  V vs. SCE), which is able to reduce the photoexcited state of 4CzIPN ( $E_{1/2}[\text{PC}^*/\text{PC}^-] = +1.35$  V vs. SCE)<sup>19</sup> to provide the EPR-observed radical anion and a transient alkyl radical of **1a**. Stern–Volmer luminescence quenching experiments (Fig. S17 and S18†) revealed efficient quenching of photoexcited 4CzIPN\* upon addition of **1a** and Cs<sub>2</sub>CO<sub>3</sub> ( $K_{\text{SV}} = 113$  M<sup>−1</sup>). *In situ* NMR studies demonstrated that **1a** react with CO<sub>2</sub> to produce compound **1d** (Scheme 4a and Fig. S20–S31,† observing the carbonic acid carbon peak), and naturally, Cs<sub>2</sub>CO<sub>3</sub> can deprotonate **1a** to give salt **1e** (Scheme 4a and Fig. S32†). While no change was observed when **1a** or **1d** was subjected to irradiation together with 4CzIPN (Fig. S33–S40†), the <sup>1</sup>H spectrum of **1e** was altered under these conditions (Fig. S41–S44†).

When the reaction of **1a** was carried out in the presence of 1 equiv. 2,2,6,6-tetramethylpiperidinyloxy (TEMPO) as a radical trap, the desired reactivity was almost completely shut down, while adducts **1f** and **1g** were formed, hinting at the presence of C(sp<sup>3</sup>)-centered alkyl radicals generated from **1a**, as well as benzoyl radicals (Scheme 4b). The detection of benzil **1i** lends further support to the formation of benzoyl radicals in the course of the reaction (Scheme 4c). Correspondingly, tri-substituted furans **1j** and **1k** were also present in the reaction mixture (Scheme 4c). It is worth noting that benzoyl radical PhC(O)• ( $E_{\text{red}} = -1.13$  V vs. SCE)<sup>20</sup> is capable of oxidizing 4CzIPN radical anion ( $E_{1/2}[\text{PC}^*/\text{PC}^-] = -1.21$  V vs. SCE),<sup>19</sup> whereas

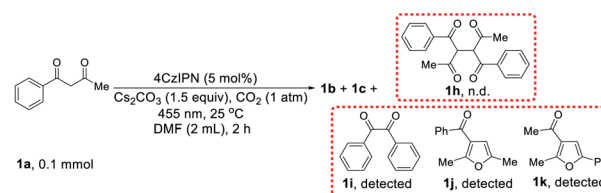
a) Reaction of **1a** with CO<sub>2</sub> or Cs<sub>2</sub>CO<sub>3</sub>



b) Reaction of **1a** with TEMPO



c) GC-MS study of the reaction mixture with **1a**



**Scheme 4** Mechanistic studies.



$\text{CH}_3\text{C}(\text{O})\cdot$  ( $E_{\text{red}} = -1.75 \text{ V vs. SCE}$ )<sup>20</sup> is not, giving a possible explanation to the lack of reactivity with acetylacetone **18a**. In addition, the dimer (**1h**) of starting material **1a** was not formed in any appreciable amount (Scheme 4c), suggesting that alkyl radicals originating from **1a** did not undergo a simple dimerization. Light “on-off” experiments indicate that the reaction needs continuous light irradiation to proceed (Fig. S19†), ruling out a radical-chain mechanism.

Based on the above observations and previous studies,<sup>7</sup> a mechanism for the  $\text{CO}_2$ -promoted photocatalytic activation of 1,3-diketones to afford tetra-substituted furans is proposed (Scheme 5). The starting material **1a** is deprotonated by  $\text{Cs}_2\text{CO}_3$  to generate enolate **1e**, which is oxidized by photoexcited  $4\text{CzIPN}^*$  through a single electron transfer process, forming  $4\text{CzIPN}^{\cdot-}$  and radical **Int2**. In addition, **1a** also equilibrates with  $\text{CO}_2$  to form adduct **1d**, which reacts with radical **Int2**, giving the dimeric **Int4**. Subsequently, **Int4** ejects benzoyl radical  $\text{PhC}(\text{O})\cdot$  (**Int5**) to form acylcyclopropane **Int6** via an intramolecular cyclization process (see ESI† section XII for discussion). Density functional theory (DFT) calculations reveal that the formation of **Int5** and **Int6** from **Int4** ( $\Delta G = +10 \text{ kcal mol}^{-1}$ , see ESI† section XIII) is most likely the rate-determining step. Thereafter, benzoyl radical **Int5** oxidizes  $4\text{CzIPN}^{\cdot-}$  to close the catalytic cycle and produce benzoyl anion **Int7**. The ring-opening rearrangement of **Int6** results in furanoid structures, **Int8** and **Int9**, via two different pathways.<sup>7c,d</sup> Computations suggest that the ring-opening processes are exergonic and favorable. The protonation and deprotonation of **Int8** and **Int9** lead to the formation of conjugated **Int10** and **Int11**. Cleavage of the C–O bonds and the accompanying nucleophilic attack by **Int7**

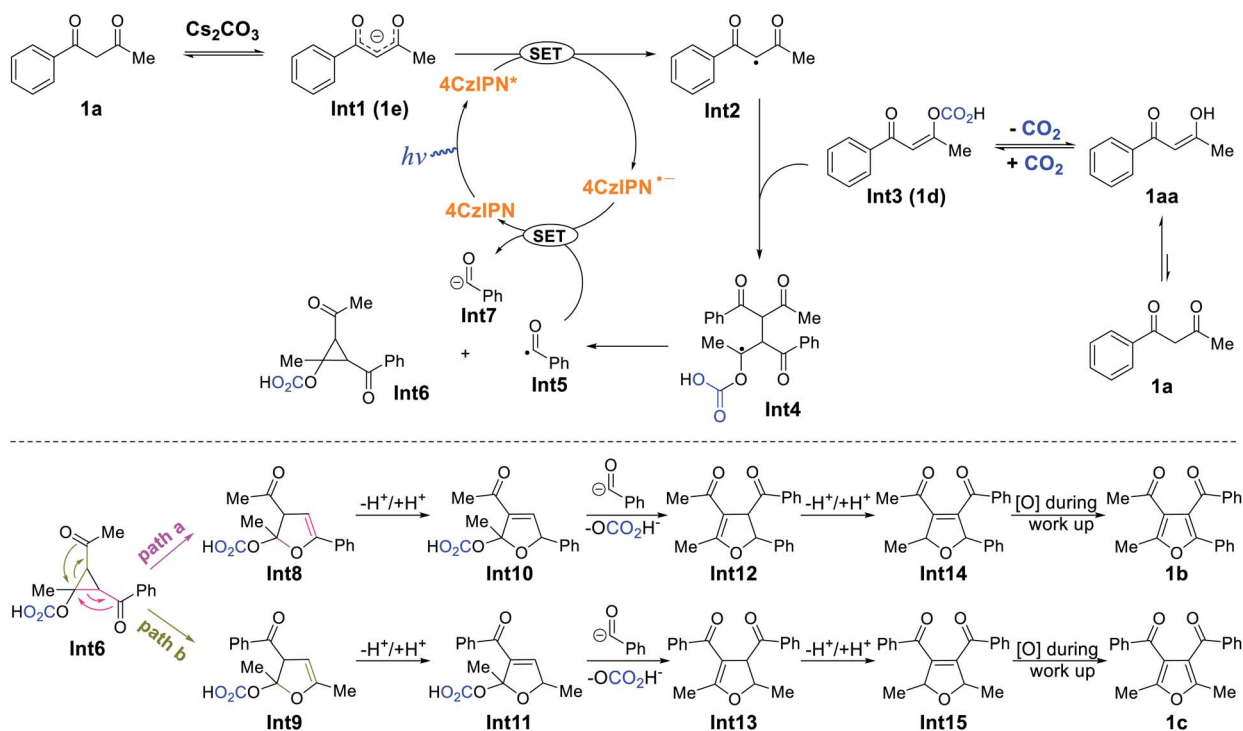
generate tetra-substituted 2,3-dihydrofurans **Int12** and **Int13** (isolated as product **16c**). We postulated that **1j** and **1k** detected by GC-MS came from the direct C–O cleavage of **Int10** and **Int11** with further aromatization in air. Intermediates **Int12** and **Int13** undergo additional protonation and deprotonation to afford the more conjugated **Int14** and **Int15** (isolated as products **16b**, **17b**, **17c**). At last, aromatization-driven oxidation processes yield the desired tetra-substituted furans.

## Conclusion

In conclusion, we have developed an unusual, transition metal-free,  $\text{CO}_2$ -promoted, visible-light-induced photocatalytic synthesis of highly substituted furan derivatives using 1,3-diketones as the only starting material. Mechanistic investigations indicated that  $\text{CO}_2$  was catalytically incorporated in order to create a better leaving group from the enolic OH group. The reaction proceeds under mild conditions via diketone radical additions and acylcyclopropane rearrangements, leading to the formation of two isomeric but differently substituted furan products. From 3-oxo-ester starting materials, partially hydrogenated furan scaffolds could also be obtained. This protocol expands the scope of the photocatalytic *de novo* synthesis of heterocyclic compounds as well as the catalytic use of  $\text{CO}_2$  as a reaction promoter.

## Data availability

All experimental, computational, and crystallographic data are available in the ESI.†



Scheme 5 Proposed reaction mechanism.



## Author contributions

Y.-M. T. and B. K. conceived the project. Y.-M. T. performed and analyzed the experiments. H. W. performed the DFT and CBS calculations. R. synthesized some materials. Y.-M. T., H. W., and B. K. prepared the manuscript. All authors discussed the results.

## Conflicts of interest

There are no conflicts to declare.

## Acknowledgements

This work was supported by the German Science Foundation (DFG) (KO 1537/18-1). This project has received funding from the European Research Council (ERC) under the European Union's Horizon 2020 Research and Innovation Programme (grant agreement 741623). We thank Dr Rudolf Vasold (University of Regensburg) for his assistance in GC-MS measurements, Regina Hoheisel (University of Regensburg) for her assistance in cyclic voltammetry measurements and Birgit Hischa (University of Regensburg) for her assistance in single crystal X-ray measurements.

## Notes and references

- (a) A. V. Gulevich, A. S. Dudnik, N. Chernyak and V. Gevorgyan, *Chem. Rev.*, 2013, **113**, 3084–3213; (b) A. Blanc, V. Bénétteau, J.-M. Weibel and P. Pale, *Org. Biomol. Chem.*, 2016, **14**, 9184–9205; (c) W. Zhang, W. Xu, F. Zhang and Y. Li, *Chin. J. Org. Chem.*, 2019, **39**, 1277–1283.
- F. Feist, *Chem. Ber.*, 1902, **35**, 1537–1545.
- V. Amarnath and K. Amarnath, *J. Org. Chem.*, 1995, **60**, 301–307.
- (a) Y. Yang, J. Yao and Y. Zhang, *Org. Lett.*, 2013, **15**, 3206–3209; (b) B. Lu, J. Wu and N. Yoshikai, *J. Am. Chem. Soc.*, 2014, **136**, 11598–11601; (c) S. Manna and A. P. Antonchick, *Org. Lett.*, 2015, **17**, 4300–4303; (d) T. Naveen, A. Deb and D. Maiti, *Angew. Chem., Int. Ed.*, 2017, **56**, 1111–1115; (e) S. Agasti, T. Pal, T. K. Achar, S. Maiti, D. Pal, S. Mandal, K. Daud, G. K. Lahiri and D. Maiti, *Angew. Chem., Int. Ed.*, 2019, **58**, 11039–11043.
- (a) K. Miki, F. Nishino, K. Ohe and S. Uemura, *J. Am. Chem. Soc.*, 2002, **124**, 5260–5261; (b) K. Miki, Y. Washitake, K. Ohe and S. Uemura, *Angew. Chem., Int. Ed.*, 2004, **43**, 1857–1860; (c) J. Barluenga, L. Riesgo, R. Vicente, L. A. López and M. Tomás, *J. Am. Chem. Soc.*, 2008, **130**, 13528–13529; (d) G. Zhang, X. Huang, G. Li and L. Zhang, *J. Am. Chem. Soc.*, 2008, **130**, 1814–1815; (e) J. González, J. González, C. Pérez-Calleja, L. A. López and R. Vicente, *Angew. Chem., Int. Ed.*, 2013, **52**, 5853–5857; (f) L. Zhou, M. Zhang, W. Li and J. Zhang, *Angew. Chem., Int. Ed.*, 2014, **53**, 5853–5857; (g) Z.-M. Zhang, P. Chen, W. Li, Y. Niu, X.-L. Zhao and J. Zhang, *Angew. Chem., Int. Ed.*, 2014, **53**, 4350–4354; (h) Y. Wang, P. Zhang, D. Qian and J. Zhang, *Angew. Chem., Int. Ed.*, 2015, **54**, 14849–14852; (i) J. S. Clark, F. Romiti, K. F. Hogg, M. H. S. A. Hamid, S. C. Richter, A. Boyer, J. C. Redman and L. J. Farrugia, *Angew. Chem., Int. Ed.*, 2015, **54**, 5744–5747; (j) M.-Y. Huang, J.-M. Yang, Y.-T. Zhao and S.-F. Zhu, *ACS Catal.*, 2019, **9**, 5353–5357.
- R. K. Shiroodi, O. Koleda and V. Gevorgyan, *J. Am. Chem. Soc.*, 2014, **136**, 13146–13149.
- (a) S. Pratapan, K. Ashok, K. R. Gopidas, N. P. Rath, P. K. Das and M. V. George, *J. Org. Chem.*, 1990, **55**, 1304–1308; (b) M. C. Sajimon, D. Ramaiah, M. Muneer, E. S. Ajithkumar, N. P. Rath and M. V. George, *J. Org. Chem.*, 1999, **64**, 6347–6352; (c) J. Barluenga, H. Fanlo, S. López and J. Flórez, *Angew. Chem., Int. Ed.*, 2007, **46**, 4136–4140; (d) J. Shao, Q. Luo, H. Bi and S. R. Wang, *Org. Lett.*, 2021, **23**, 459–463; (e) X. He, Y. Tang, Y. Wang, J.-B. Chen, S. Xu, J. Dou and Y. Li, *Angew. Chem., Int. Ed.*, 2019, **58**, 10698–10702.
- H. Jin and A. Fürstner, *Angew. Chem., Int. Ed.*, 2020, **59**, 13618–13622.
- (a) T. Sakakura, J.-C. Choi and H. Yasuda, *Chem. Rev.*, 2007, **107**, 2365–2387; (b) Q. Liu, L. Wu, R. Jackstell and M. Beller, *Nat. Commun.*, 2015, **6**, 5933–5948; (c) X. He, L.-Q. Qiu, W.-J. Wang, K.-H. Chen and L.-N. He, *Green Chem.*, 2020, **22**, 7301–7320; (d) Z. Zhang, J.-H. Ye, T. Ju, L.-L. Liao, H. Huang, Y.-Y. Gui, W.-J. Zhou and D.-G. Yu, *ACS Catal.*, 2020, **10**, 10871–10885; (e) Z. Fan, Z. Zhang and C. Xi, *ChemSusChem*, 2020, **13**, 6201–6218; (f) J.-H. Ye, T. Ju, H. Huang, L.-L. Liao and D.-G. Yu, *Acc. Chem. Res.*, 2021, **54**, 2518–2531; (g) B. Cai, H. W. Cheo, T. Liu and J. Wu, *Angew. Chem., Int. Ed.*, 2021, **60**, 18950–18980.
- (a) C.-J. Li and B. M. Trost, *Proc. Natl. Acad. Sci. U. S. A.*, 2008, **105**, 13197–13202; (b) D. Riemer, B. Mandaviya, W. Schilling, A. C. Götz, T. Kühn, M. Finger and S. Das, *ACS Catal.*, 2018, **8**, 3030–3034; (c) D. Riemer, W. Schilling, A. Goetz, Y. Zhang, S. Gehrke, I. Tkach, O. Hollóczki and S. Das, *ACS Catal.*, 2018, **8**, 11679–11687.
- (a) P. Braunstein, D. Matt and D. Nobel, *Chem. Rev.*, 1988, **88**, 747–764; (b) T. Sakakura and K. Kohno, *Chem. Commun.*, 2009, 1312–1330; (c) K. Huang, C.-L. Sun and Z.-J. Shi, *Chem. Soc. Rev.*, 2011, **40**, 2435–2452; (d) R. Martín and A. W. Kleij, *ChemSusChem*, 2011, **4**, 1259–1263; (e) Y. Tsuji and T. Fujihara, *Chem. Commun.*, 2012, **48**, 9956–9964; (f) P. G. Jessop, S. M. Mercer and D. J. Heldebrant, *Energy Environ. Sci.*, 2012, **5**, 7240–7253; (g) S. B. Lang, T. M. Locascio and J. A. Tunge, *Org. Lett.*, 2014, **16**, 4308–4311; (h) F. D. Bobbink and P. J. Dyson, *J. Catal.*, 2016, **343**, 52–61; (i) M. Börjesson, T. Moragas, D. Gallego and R. Martin, *ACS Catal.*, 2016, **6**, 6739–6749; (j) S. Wang, G. Du and C. Xi, *Org. Biomol. Chem.*, 2016, **14**, 3666–3676; (k) P. Hirapara, D. Riemer, N. Hazra, J. Gajera, M. Finger and S. Das, *Green Chem.*, 2017, **19**, 5356–5360; (l) W. Schilling and S. Das, *Tetrahedron Lett.*, 2018, **59**, 3821–3828; (m) Z. Zhang, J.-H. Ye, D.-S. Wu, Y.-Q. Zhou and D.-G. Yu, *Chem.-Asian J.*, 2018, **13**, 2292–2307; (n) A. Tortajada, F. Juliá-Hernández, M. Börjesson, T. Moragas and R. Martin, *Angew. Chem., Int. Ed.*, 2018, **57**, 15948–15982; (o) L. Wang, W. Sun and C. Liu, *Chin. J. Chem.*, 2018, **36**, 353–362; (p) Y. Cao, X. He, N. Wang, H.-R. Li and L.-N. He, *Chin. J. Chem.*, 2018, **36**, 644–659; (q) C. S. Yeung,



- Angew. Chem., Int. Ed.*, 2019, **58**, 5492–5502; (r) Q.-Y. Meng, T. E. Schirmer, A. L. Berger, K. Donabauer and B. König, *J. Am. Chem. Soc.*, 2019, **141**, 11393–11397; (s) M. Schmalzbauer, T. D. Svejstrup, F. Fricke, P. Brandt, M. J. Johansson, G. Bergonzini and B. König, *Chem*, 2020, **6**, 2658–2672; (t) S. Wang, B.-Y. Cheng, M. Sršen and B. König, *J. Am. Chem. Soc.*, 2020, **142**, 7524–7531; (u) Y. Zhang, T. Zhang and S. Das, *Green Chem.*, 2020, **22**, 1800–1820; (v) K. Donabauer and B. König, *Acc. Chem. Res.*, 2021, **54**, 242–252; (w) R. Cauwenbergh and S. Das, *Green Chem.*, 2021, **23**, 2553–2574; (x) P. K. Sahoo, Y. Zhang and S. Das, *ACS Catal.*, 2021, **11**, 3414–3442.
- 12 E. F. Lutz (Shell Oil Co.), *US Pat.* 3518310A, 1970.
- 13 Y. Sugawara, W. Yamada, S. Yoshida, T. Ikeno and T. Yamada, *J. Am. Chem. Soc.*, 2007, **129**, 12902–12903.
- 14 J. Ye, I. Kalvet, F. Schoenebeck and T. Rovis, *Nat. Chem.*, 2018, **10**, 1037–1041.
- 15 M. Kapoor, P. Chand-Thakuri and M. C. Young, *J. Am. Chem. Soc.*, 2019, **141**, 7980–7989.
- 16 (a) J. Song, H. Zhang, X. Chen, X. Li and D. Xu, *Synth. Commun.*, 2010, **40**, 1847–1855; (b) Y. Yue, Y. Zhang, W. Song, X. Zhang, J. Liu and K. Zhuo, *Adv. Synth. Catal.*, 2014, **356**, 2459–2464; (c) P.-J. Zhou, C.-K. Li, S.-F. Zhou, A. Shoberu and J. P. Zou, *Org. Biomol. Chem.*, 2017, **15**, 2629–2637.
- 17 (a) C. He, S. Guo, J. Ke, J. Hao, H. Xu, H. Chen and A. Lei, *J. Am. Chem. Soc.*, 2012, **134**, 5766–5769; (b) Y. Ma, S. Zhang, S. Yang, F. Song and J. You, *Angew. Chem., Int. Ed.*, 2014, **53**, 7870–7874.
- 18 For the EPR signals of similar isophthalonitrile species, see: (a) E. W. Evans, Y. Olivier, Y. Puttisong, W. K. Myers, T. J. H. Hele, S. M. Menke, T. H. Thomas, D. Credgington, D. Beljonne, R. H. Friend and N. C. Greenham, *J. Phys. Chem. Lett.*, 2018, **9**, 4053–4058; (b) J. Xu, J. Cao, X. Wu, H. Wang, X. Yang, X. Tang, R. W. Toh, R. Zhou, E. K. L. Yeow and J. Wu, *J. Am. Chem. Soc.*, 2021, **143**, 13266–13273.
- 19 T.-Y. Shang, L.-H. Lu, Z. Cao, Y. Liu, W.-M. He and B. Yu, *Chem. Commun.*, 2019, **55**, 5408–5419.
- 20 C. Chatgililoglu, D. Crich, M. Komatsu and I. Ryu, *Chem. Rev.*, 1999, **99**, 1991–2069.

